Received: 13 February 2022 | Revised: 01 April 2022 | Accepted: 06 April 2022
DOI: 10.22034/ecc.2022.333898.1374
Eurasian Chemical Communications
SAMI

FULL PAPER

Density functional theory, ADME and docking studies of some tetrahydropyrimidine-5-carboxylate derivatives

Ali Majeed Hantoush[a] |Zaheda Ahmed Najim[b] |Faris T. Abachi[c,*]

[a]*Department of Pharmaceutical Chemistry, College of Pharmacy, University of Albayan, Baghdad, Iraq*

[b]*Department of Chemistry, College of Education of Pure Science, University of Mosul, Mosul, Iraq*

[c]*Department of Pharmaceutical Chemistry, College of Pharmacy, University of Mosul, Mosul, Iraq*

***Corresponding Author:**
Faris T. Abachi
Email: Faris_abachi@uomosul.edu.iq
Tel.: +9647703336180

Pyrimidine derivatives have a wide application. These derivatives act as dihydrofolate reductase inhibitors, and are an important class of drugs, as evidenced by their usage as anti-microbial, anti-malarial, and anti-cancer agents. The aim of this study was to design a new series of tetrahydropyrimidine-5-carboxylate derivatives as anti-bacterial dihydrofolate reductase [DHFR] inhibitors using density functional theory [DFT] studies and molecular docking against two enzymes DHFR inhibitors and DNAgyrase. Also, the pharmacokinetic parameters absorption, distribution, metabolism, and excretion [ADME] were predicated. The scores of the docking studies showed all compounds have good interactions with the [DHFR] as well as drug likeness.

KEYWORDS

DHFR inhibitors; DFT studies; pyrimidine derivatives; ADME.

Introduction

Several pyrimidine derivatives are associated with pharmaceutical and biological activities including antibacterial [1], antifungal [2], antileishmanial [3], anti-inflammatory [4], analgesics [5], natural products (such as nucleotides, nucleic acids, vitamins, pterins, and antibiotics) [6], antihypertensive [7], antiviral [8], anti-diabetic [9], anti-allergic [10], anticonvulsant [11], antioxidant [12], antihistaminic [13], herbicidal [14], anticancer activities [15]. Many pyrimidine derivatives have been shown to have possible central nervous system (CNS), depressant properties [16], as well as calcium channel blocker qualities [17].

Computer-aided drug design, in particular protein-ligand docking, has brought about the discovery of many biologically active drugs [18,19]. In many enzyme-ligand docking programs, a flexible small organic molecule structure is docked in a rigid protein (enzyme) receptor structure in order to find the optimal binding conformation and affinity of the small molecule within the protein binding pocket.

Non-classical dihydrofolate reductase inhibitors are pyrimidine derivatives. For a long time, inhibitors of dihydrofolate reductase [DHFR], an enzyme that catalyzes 5,6,7,8-tetrahydrofolate synthesis, have been employed as antibacterial and antimetabolite agents (such as methotrexate) [15].

The pyrimidine ring is a four-carbon aromatic heterocycle with two nitrogen atoms. Pyrimidines are single as well as fused rings that seem to be structural components in many natural compounds and drugs. The atomic charges of any and all exocyclic atoms correlate to their electro-negativity, whereas the charges of all carbon atoms in the ring are corresponded to the net flow of electrons (electron delocalization) [20].

Molecular docking, on the other hand, is a useful and widely used technique in drug design. It is a computational procedure to predict the binding affinity between a small molecule (ligand) and a macromolecule (receptor), which is very essential in drug development. A molecular docking study on the evaluation of potential antibacterial agents was published recently. Some scoring functions predict the biological and complementary activity of the ligand. For most cases, docking scores are more important than having an exact position [21]. In this study, we use computational approaches (DFT) and docking to design new series of tetrahydropyrimidine derivatives as folate reductase inhibitors, particularly those are dependent on receptor superposition (rather than ligand superposition), such as docking root mean square deviation (RMSD), likewise to predict their physicochemical features, pharmacokinetic parameters (ADME).

Calculation of the electronic structure using DFT

The GAUSSIAN 09 suite of programs was used to execute all of the computational calculations [22]. The DFT/B3LYP level of theory and molecular mechanics are used to optimize the molecular geometry of pyrimidine derivatives compounds A1–A6 (methotrexate as a reference). Strain energy values were estimated using MM2 methods [23]. The Lee-Yang-Parr correlation functional (B3LYP) is a relatively recent DFT functional that has shown a lot of promise in molecular simulations of organic molecules. The global minimum structures of our optimized compounds were later confirmed by frequency calculations for six selected compounds as shown in Table 1.

The 3D optimized geometry and its single crystal structure provide the good information about the comparison of bond lengths, the optimal bond angles, Van Der Waals forces, and dipole-dipole interactions, as well as experimental geometries and reveal a reasonable agreement, demonstrating the dependability of our computational method in this study [24]**.** The energy gap between the highest occupied molecular orbitals (HOMOs) and the lowest unoccupied molecular orbitals (LUMOs) is known as the frontier molecular orbitals [25]. The prepared 3D structures were then optimized to acquire an energetically stable conformation.

Physicochemical, pharmacokinetic, ADME prediction and drug-Likeness

Table 2 shows the computed molecular characteristics of Lipinski's rule of five, which were determined using SwissADME online (http://swissadme) non-defined [26]. As a result, the Lipinski rule of five was used to construct hundreds of 3-D structures of novel pyrimidine derivatives and forecast their physicochemical features. The pharmacokinetics and drug-likeness characteristics were also calculated; only four compounds were fixed in this study as models.

Molecular docking

Dihydrofolate reductase (DHFR) and DNAgyrase-II were chosen as the enzymes to study in this research project. The computational docking study was carried out using the online platform Mcule. The interaction to generate a pyrimidine-enzyme complex reflects the docking of these molecules ligands and enzymes. The results showed that the pyrimidine-DHFR has a high score whereas the pyrimidine-DNAgyrase-II has a low score. Figures 2 and 3 illustrate the 2D and 3D interactions of compounds 1-6 with dihydrofolate reductase (DHFR) (1hfr) and DNA gyrase-II, respectively [27]. A common metric used to evaluate distance between the predicated pose and the native

pose, given a superposition of their protein receptor 3D structures, as represented in the equation.

$$RMSD = \sqrt{1/N}\sum_{i=1}^{N} di^{2}$$

In which, N is the number of atoms in the ligand, d is the distance the i^{th} pair of the corresponding atoms.

Results

Different protocols were used for the synthesis of tetrhydropyrimidine derivatives. To study the chemical stability, the electronic charges of π electrons are delocalized around Exo, and Endo design pyrimidine ring atoms can be determined theoretically [21]. The DFT-B3LYP descriptors were determined to understand the structure and reactivity of four designated pyrimidine analogous (A1-A4) molecules, the reactivity parameters include energy gab, charges at the π-bond carbon atoms in pyrimidine ring (C5, C6) and π-bond order. The calculated values of the mentioned parameters are analogous (A1-A6) Table (1) [20].

TABLE 1 Summary of reactivity descriptors at the DFT/B3LY theory level

Comp. No	E_{homo} (kcal/mole)	E_{lumo} (kcal/mole)	ΔE* (kcal/mole)	Strain Energ (kcal/mole)	ΔH_f (kcal/mole)
1	-0.3254	0.1039	0.4293	4.1531	-67.5099
2	-0.3102	0.0976	0.4078	3.1123	-124.8058
3	-0.3290	0.0925	0.4215	4.1146	-125.628
4	-0.3166	0.0767	0.3933	11.6953	-26.3
5	-0.3093	0.0775	0.3868	10.5383	-70.7468
6	-0.3158	0.0957	0.4115	11.5720	-71.5371
MXT	-0.2973	0.0594	0.3567	44.3876	-86.5578

*$\Delta E = E_{homo} - E_{lumo}$

The larger energy gab ($\Delta E = |E_{HOMO}| - |E_{LUMO}|$) indicated that all six selected molecules have the similar energy, more stable, and have less reactivity [26].

For a detailed study of the determined physicochemical parameters the rule of five was used (Table 2).

TABLE 2 Lipinski's rule of five (Ro5) for the tetrhydo pyrimidine derivatives

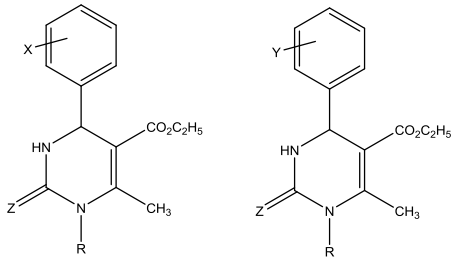

No.	X/R	Y	Z	M.F	M.Wt 500<	H.B don < 5	H.B acc ≤10	ClogP < 4.5	BBB
1	H/H	-	O	$C_{14}H_{16}N_2O_3$	260	2	3	1.56	NO
2	OH/H	-	O	$C_{14}H_{16}N_2O_3$	276	3	4	1.14	NO
3	NH_2 /H	-	O	$C_{14}H_{17}N_3O_3$	275	3	3	1.00	NO
4	CH_3/H	-	O	$C_{15}H_{18}N_2O_3$	274	2	3	1.88	NO
5	NO_2/H	-	O	$C_{14}H_{13}5N_3O_5$	305	2	3	0.81	NO
6	F/H	-	O	$C_{14}H_{15}FN_2O_3$	278	2	4	1.86	YES

7	Cl/H	-	O	$C_{14}H_{15}ClN_2O_3$	294	2	3	2.09	YES
8	Br/H	-	O	$C_{14}H_{15}BrN_2O_3$	339	2	3	2.18	YES
9	I/H	-	O	$C_{14}H_{15}IN_2O_3$	386	2	3	2.22	YES
10	H/CH_3	-	O	$C_{15}H_{18}N_2O_3$	274	1	3	1.75	YES
11	OH/CH_3	-	O	$C_{15}H18N_2O_4$	290	2	4	1.37	NO
12	NH_2/CH_3	-	O	$C_{15}H_{19}N_3O_3$	289	2	3	1.21	NO
13	CH_3/CH_3	-	O	$C_{16}H_{20}N_2O_3$	288	1	3	2.09	YES
14	NO_2/CH_3	-	O	$C_{15}H_{17}N_3O_5$	319	1	5	1.00	NO
15	F/CH_3	-	O	$C_{15}H_{17}FN_2O_3$	292	1	4	2.08	YES
16	Cl/CH_3	-	O	$C_{15}H_{17}ClN_2O_3$	308	1	3	2.30	YES
17	Br/ CH_3	-	O	$C_{15}H_{17}BrN_2O_3$	353	1	3	2.37	YES
18	I/ CH_3	-	O	$C_{15}H_{17}IN_2O_3$	400	1	3	2.41	YES
19	-	H/H	S	$C_{14}H_{16}N_2O_2S$	276	2	2	2.07	NO
20	-	OH/ H	S	$C_{14}H_{16}N_2O_3S$	292	3	3	1.65	YES
21	-	NH_2/ H	S	$C_{14}H_{17}N_3O_2S$	291	3	2	1.51	NO
22	-	CH_3/ H	S	$C_{15}H_{18}N_2O_2S$	290	2	2	2.38	NO
23	-	NO_2/ H	S	$C_{14}H_{15}N_3O_4S$	321	2	4	1.30	NO
24	-	F/H	S	$C_{14}H1_5FN_2O_2S$	294	2	3	2.38	NO
25	-	Cl/H	S	$C_{14}H_{15}ClN_2O_2S$	310	2	2	2.61	NO
26	-	Br/H	S	$C_{14}H_{15}BrN_2O2S$	355	2	2	2.69	NO
27	-	I/H	S	$C_{14}H_{15}IN_2O_2S$	402	2	2	2.74	NO
28	-	H/CH_3	S	$C_{15}H_{18}N_2O_2S$	290	1	2	2.25	NO
29	-	OH/CH_3	S	$C_{15}H_{18}N_2O_3S$	306	2	3	1.84	NO
30	-	NH_2/ CH_3	S	$C_{15}H_{19}N_3O_2S$	305	2	2	1.74	NO
31	-	CH_3/ CH_3	S	$C_{16}H_{20}N_2O_2S$	304	1	2	2.50	NO
32	-	NO_2/ CH_3	S	$C_{15}H_{17}N_3O_4S$	335	1	4	1.52	NO
33	-	F/ CH_3	S	$C_{15}H_{17}FN_2O_2S$	308	1	3	2.58	YES
34	-	Cl/ CH_3	S	$C_{15}H_{17}ClN_2O_2S$	324	1	2	2.80	YES
35	-	Br/ CH_3	S	$C_{15}H_{17}BrN_2O_2S$	369	1	2	2.87	YES
36	-	I/ CH_3	S	$C_{15}H1_7IN_2O_2S$	416	1	2	2.91	YES

MWt: Molecular weight; calculated lipophilicity (Clog P o/w); Number of hydrogen bond donors ($H.B_{don}$); Number of hydrogen bond acceptors ($H.B._{acc}$).

The Lipinski Rule of Five is followed by all compounds A1-A36 Table (2) [28]. They also follow additional rules like (Ghose, Veber, Egan, and Muegge) [29-31].

The web (http://swissadme) was used to calculate the pharmacokinetic characteristics of these tetrahydopyrimidine derivatives. All these derivatives are not blood brain barrier except the compounds (6-10, 15-18, 20, and 33-36) are blood brain barrier, mostly of these derivatives have hydroxyl or halogen on the aromatic ring. When a methyl group in nitrogen (N1) is replaced, all of the compounds demonstrate substantial absorption from the GI tract and do not penetrate the blood-brain barrier (BBB) except the substituted phenyl with hydroxyl (OH) or halogenated agents (F, Cl, Br, and I). This may be due to increased lipophilicity [32]. This sort of molecule containing aryl groups was also predicted as (BBB), which is essential in the research of pyrimidine and its derivatives' quantitative structure-activity relationships (QSAR).

The predicted metabolic values for compounds (1-36) by using five major cytochromes P-450, CYP isoforms, only few agents are active against (CYP2C19, CYP2C9) [33].

In the preclinical stage, on the numerical prediction of P-glycoprotein substrate mediated the drug-drug interaction (DDI) and nonlinear absorption *in vivo* [34]. In the prediction of drug transport properties for compounds 1-36, the molecular polar surface area (TPSA (A^2)) is an important parameter [27,35].

TABLE 3 Drug likeness calculations of the selected compounds 1-36

Compd. No.	TPSA (oA2)	% ABS 109-(0.345 x TPSA)	Drug Likeness
1	67.43	85.73	Yes
2	89.66	78.0673	Yes
3	93.45	76.7597	Yes
4	67.43	85.73	Yes
5	112.25	70.2737	Yes
6	67.43	85.73	Yes
7	67.43	85.73	Yes
8	67.43	85.73	Yes
9	67.43	85.73	Yes
10	58.64	88.7692	Yes
11	78.87	81.7898	Yes
12	84.66	79.7923	Yes
13	58.64	88.7692	Yes
14	104.46	36.0387	Yes
15	58.64	88.7692	Yes
16	58.64	88.7692	Yes
17	58.64	88.7692	Yes
18	58.64	88.7692	Yes
19	82.45	80.5547	Yes
20	102.68	73.5754	Yes
21	108.47	71.5778	Yes
22	82.45	80.5547	Yes
23	128.27	64.7468	Yes
24	82.45	80.5547	Yes
25	82.45	80.5547	Yes
26	82.45	80.5547	Yes
27	82.45	80.5547	Yes
28	73.66	83.5873	Yes
29	93.89	76.6079	Yes

30	99.68	74.5379	Yes
31	73.66	83.5873	Yes
32	119.48	67.7794	Yes
33	73.66	83.5873	Yes
34	73.66	83.5873	Yes
35	73.66	83.5873	Yes
36	73.66	83.5873	Yes

The computation of the molecular polar surface, on the other hand, takes a long time due to the need to produce a reasonable 3-D molecular geometry and the calculation of the surface as a good indication of drug-likeness for all compounds (Table 3) [36-38].

In silico development of receptors and ligands, docking, and validation all were involved in the molecular modeling studies. A thorough description of the method can be found elsewhere. In summary, the PDB (PDB ID: 1hfr) gave a high-resolution human DHFR structure extending and DNA gyrase (II). The addition of hydrogen and charges to the receptor structure primed it for docking. Since docking to receptor ensembles was explained in (Tables 4 and 5) [39].

TABLE 4 Molecular docking of compounds A1-A6 against DHFR enzyme

Comp. No.	Ligand-DHFR (1hfr) Interaction 2D structure	3D structure	Binding energy kcal/mole	RMSD
1		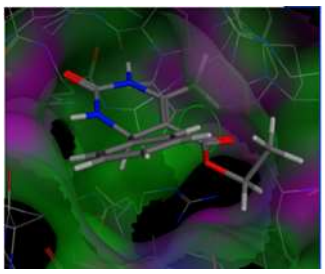	-9.8264	0.800
2		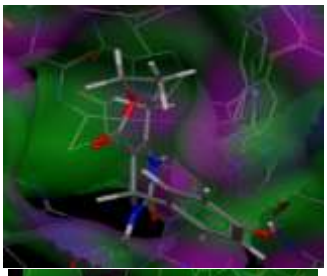	-11.3735	0.400
3		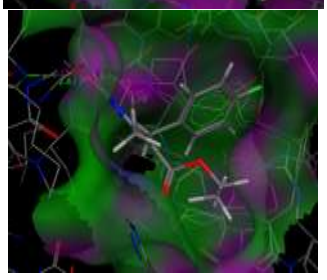	-9.8806	0.000

4		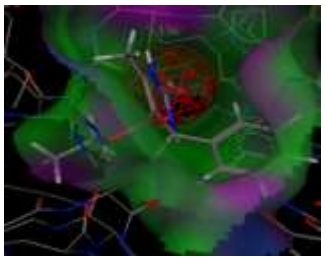	-10.8541	1.400
5		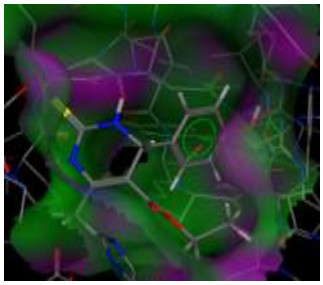	-11.4459	1.980
6		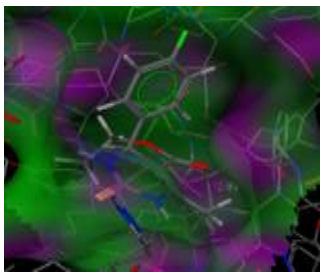	-10.7208	1.8113
Ref. (MTX)	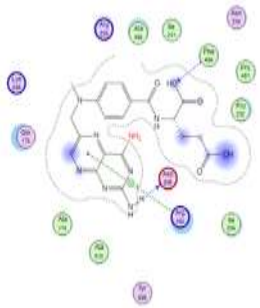	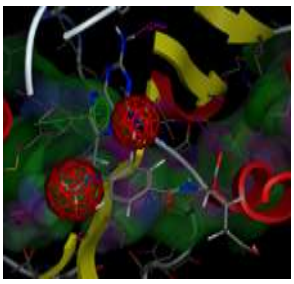	-14.64	1.00

TABLE 5 Molecular docking of compounds A1-A6 against DNAgyrase-II enzyme

Comp. No.	Ligand –DNAgyrase-II Interaction	3D structure	Binding energy Kcal/mole	RMSD
1		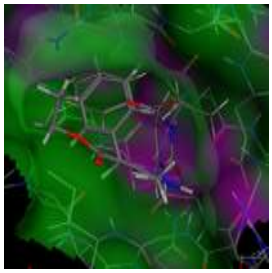	-9.7922	1.2

2	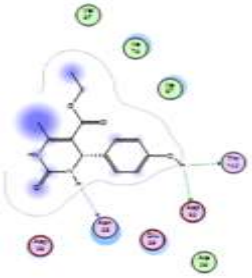	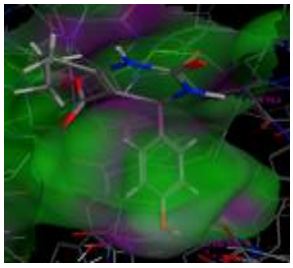	-10.5435	0.400
3		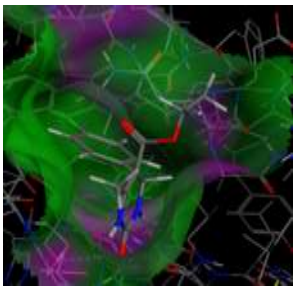	-10.4035	1.2
4	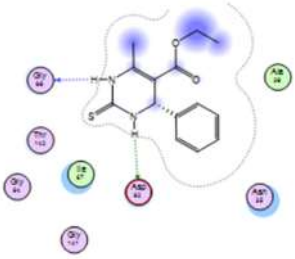	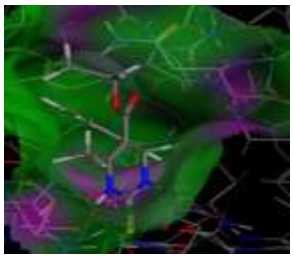	-9.7191	1.80
5	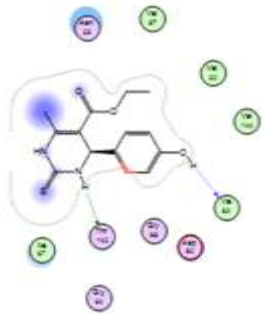	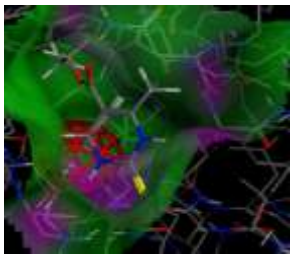	-11.6553	1.428
6		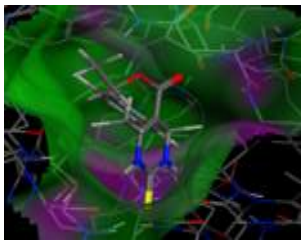	-9.4466	1.255

Ref.	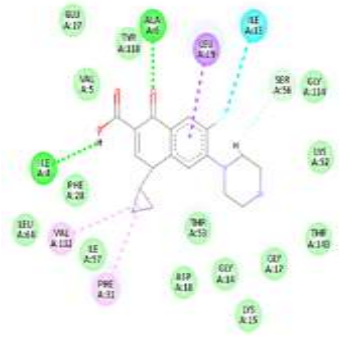	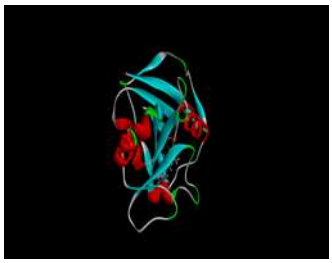	-9.4000	1.00
	Ciprofloxacin			

Discussion

The results demonstrated that quantum chemical calculations of the tetrahyropyrimidine molecule employing charge, bond order, and energy calculations of the exciting characteristics of the pyrimidine nucleus use DFT calculations with the standard DFT-B3LYP. The precision of DFT calculations was cited as a factor in the selection of the functional and basis sets. The quantum chemical descriptors obtained using DFT calculations are shown in (Table 1) [22].

Frontier molecular orbital energies (FMOE) are crucial characteristics in a variety of chemical and pharmacological processes. The electron-donating character of a chemical is measured by E_{HOMO}, while the electron absorbing character is measured by E_{LUMO}. The stability of tetrahydropyrimidine derivatives was further investigated using DFT calculations. The total energy E is the same in the six selected molecules as a model, more stable, based on the previous conclusions for reference compound (methotrexate). As a result, the decrease of the HOMO-LUMO energy gap is mostly a result of the LUMO's significant stability due to the electron-acceptor group's strong electron accepting capability, which affects the molecule's biological activity as compared with methotrexate as a reference molecule [28].

Furthermore, examinations of the hundred compounds, and select the compounds 1-36 *in silico* projected physicochemical, pharmacokinetic, ADME characteristics, and drug-likeness demonstrated that they meet Lipinski's rule requirements and have good drug score values (table 2). By inserting a methyl group in position 3 of the pyrimidine ring (-N-CH_3) and comparing it with the compounds with no methyl-substituted (-N-H), the substituted (N-CH_3) series penetrates the blood-brain barrier (BBB), but compounds with no methyl-substituted (-N-H) compounds do not [34].

The importance of QSAR investigations of tetrahyropyrimidine derivatives having various groups is demonstrated by these positive results (donating and withdrawing groups). All computed drug-likeness scores for compounds 1-36 are listed in (Table 3) and are drug-likeness [36].

Two enzymes dihyrofolate reductase inhibitors (1hfr) and DNA-grase were evaluated using molecular docking analysis in 2-D and 3-D structures using methatroxate (MXT) and ciprofloxacin as references. The score of the docking ligand with the DHFD (1hfr) were showed lower values than the MTX. While, the same compounds were showed higher score values than ciprofloxacin (Table 5).

The lowest binding energies of the selected molecules (A1-A4) were found to range from –10.526 to –9.350 kcal/mole, with less energy in the case of DNA-gyrase II, as depicted in (Table 4) and (Figures 2 and 3) [27,38]. The docking and kind of these interactions are explained using the 2-D and

3-D structures of the designated pyrimidine chemical structures of the ligands with the selected enzyme interactions [39]. The pyrimidine nucleus and the DHFR (1hfr) enzyme have lower binding scores than DNA-gyrase [39-42]. Moreover, the docking results demonstrated that as the hydrophobic substitution increased in the tested tetrhydropyrimidine derivatives the scores will increases, too. Further studies were needed to prepare the active compound and evaluate its antimicrobial activity.

To examine the impact of symmetry correction in docking RMSD calculation relative to the native score ≤ 2.0 Å, one would anticipate the RMSD value should be low, these values do not reflect correct corresponding of the atomic mapping derived from the tetrhydropyrimidine derivatives (ligand) bonding 3D structures [26,43].

Conclusion

In conclusion, the biological potential of pyrimidine and its derivatives as an important nucleus in natural and synthetic agents, new series of tetrahydropyrimidine was designated as Dihydrofolate reductase inhibitors, DNAgyrase, docking, and theoretical study their physicochemical properties were discussed thoroughly.

Acknowledgements

Our thanks to Departments of Pharmaceutical Chemistry, Colleges of Pharmacy, Mosul & Baghdad Universities, and Department of Chemistry, College of Education for Pure Science, University of Mosul.

Conflict of interests

There are no conflicts of interest declared by the author.

Funding

This study received no funding from government, commercial, or non-profit organizations.

Orcid:

Faris T. Abachi:
https://www.orcid.org/0000-0003-3389-877X

References

[1] N.E. Abd El-Sattar, K. El-Adl, M.A. El-Hashash, S.A. Salama, M.M. Elhady, *Bioorg. Chem.*, **2021**, *115*, 105186. [Crossref], [Google Scholar], [Publisher]

[2] W. Wu, W. Lan, C. Wu, Q. Fei, *Front. Chem.*, **2021**, *9*, 695628. [Crossref], [Google Scholar], [Publisher]

[3] H. Istanbullu, G. Bayraktar, H. Akbaba, I. Cavus, G. Coban, B.D. Butuner, A. Ahmet Kilimcioglu, A. Ozbilgin, V. Alptuzun, E. Erciyas, *Archiv der Pharmazie*, **2020**, *353*, 1900325. [Crossref], [Google Scholar], [Publisher]

[4] H. ur Rashid, M.A.U. Martines, A.P. Duarte, J. Jorge, S. Rasool, R. Muhammad, N. Ahmad, M.N. Umar, *RSC Adv.*, **2021**, *11*, 6060-6098. [Crossref], [Google Scholar], [Publisher]

[5] D. Kalpana, S. Rekha, V. Murugan, H. Shivaprakash, *Res. J. Pharm. Tech.*, **2021**, *14*, 2529-5234. [Crossref], [Google Scholar], [Publisher]

[6] P.V. Zadorozhnii, V.V. Kiselev, N.O. Teslenko, A.V. Kharchenko, I.O. Pokotylo, O.V. Okhtina, O.V. Kryshchyk, *Res. J. Pharm. Tech.*, **2017**, *10*, 3957-3963. [Crossref], [Google Scholar], [Publisher]

[7] N. Irshad, A. Khan, M.S. Iqbal, *Biomed. Pharmacother.*, **2021**, *139*, 111567. [Crossref], [Google Scholar], [Publisher]

[8] K.I. Bhat, A. Kumar, P. Kumar, E.K. Riyaz, *Research J. Pharm. and Tech.*, **2014**, *7*, 995-998. [Google Scholar], [Publisher]

[9] F. Bassyouni, M. Tarek, A. Salama, B. Ibrahim, S.S. El Dine, N. Yassin, A. Hassanein, M. Moharam, M. Abdel-Rehim, *Molecules*, **2021**, *26*, 2370. [Crossref], [Google Scholar], [Publisher]

[10] M. Devi, S. Jaiswal, J. Dwivedi, N. Kaur, *Curr. Org. Chem.*, **2021**, *25*, 2625-2649. [Crossref], [Google Scholar], [Publisher]

[11] H.I. Severina, O.O. Skupa, N.I. Voloshchuk, M.M. Suleiman, V.A. Georgiyants, *Pharmacia*, **2019**, *66*, 141-146. [Crossref], [Google Scholar], [Publisher]
[12] S. Chauhan, A.K. Gyananchandran, P. Tiwari, S. Sharma, S.S. Shukla., *Research J. Pharm. Tech*., **2011**, *4*, 624-628. [Google Scholar], [Publisher]
[13] M. Grosicki, K.H. Kieć-Kononowicz, *Curr. Med Chem.*, **2015**, *22*, 2087-2099. [Google Scholar], [Publisher]
[14] R. Yadav, P. Srivastava, *Research J. Pharm. Tech.*, **2019**, *12*, 584-588. [Crossref], [Google Scholar], [Publisher]
[15] B. Tylińska, B. Wiatrak, Ż. Czyżnikowska, A. Cieśla-Niechwiadowicz, E. Gębarowska, A. Janicka-Kłos, *Int. J. Mol. Sci.*, **2021**, *22*, 3825. [Crossref], [Google Scholar], [Publisher]
[16] K. Marek, G. Ślifirski, J. Kleps, S. Ulenberg, M. Belka, T. Bączek, A. Siwek, K. Stachowicz, B. Szewczyk, G. Nowak, B. Duszyńska, F. Herold, *Int. J. Mol. Sci.*, **2021**, *22*, 2329. [Crossref], [Google Scholar], [Publisher]
[17] S. Mahgoub, M.I.K. El-Sayed, M.F. El-Shehry, S.M. Awad, Y.E. Mansour, S.S. Fatahala, *Bioorg. Chem.*, **2021**, *116*, 105272. [Crossref], [Google Scholar], [Publisher]
[18] T. Tuccinardi, *Comb. Chem. High Throughput Screen.*, **2009**, *12*, 303-314. [Crossref], [Google Scholar], [Publisher]
[19] P. Śledź, A. Caflisch, *Curr. Opin. Struct. Biol.*, **2018**, *48*, 93-102. [Crossref], [Google Scholar], [Publisher]
[20] A. Manlove, M.P. Groziak, *Prog. Heterocycl. Chem.*, **2009**, *21*, 375–414. [Crossref], [Google Scholar], [Publisher]
[21] T.N. Lohith, L. Kumar, R. Verma, *Research J. Pharm. Tech.*, **2020**, *13*, 1899-1904. [Crossref], [Google Scholar], [Publisher]
[22] M.J. Frisch, G.W. Trucks, H.B. Schlegel, G.E. Scuseria, M.A. Robb, J.R. Cheeseman, D.J. Fox, Gaussian 09, Revision D.01. GaussianInc., **2013**, 1–20.
[23] R.O. Jones, *Rev. Mod. Phys.*, **2015**, *87*, 897–923. [Crossref], [Google Scholar], [Publisher]
[24] Z.H. Al-Sawaff, Z.A. Najim, S. Sabeeh, F. Kandemirli, *Solid State Technol.*, **2020**, *63*, 5443-5449. [Google Scholar], [Publisher]
[25] G. Gece, *Corros. Sci.*, **2008**, *50*, 2981–2992. [Crossref], [Google Scholar], [Publisher]
[26] E.W. Bell, Y. Zhang, *J. Cheminform.*, **2019**, *11*, 40. [Crossref], [Google Scholar], [Publisher]
[27] Z.A. Najim, *Egypt. J. Chem.*, **2021**, *64*, 3457–3463. [Crossref], [Google Scholar], [Publisher]
[28] A. Daian, O. Michielin, V. Zoete, *J. Chem. Info. Mod.*, **2014**, *54*, 3284-3301. [Crossref], [Google Scholar], [Publisher]
[29] D.D. Kodical, J.P. James, D.K, P. Kumar, C. Cyriac, K.V. Gopika, *Research J. Pharm. Tech.*, **2020**, *13*, 4200-4206. [Crossref], [Google Scholar], [Publisher]
[30] S. Murugavel, S. Vijayakumar, *S. Nagarajan, A. Ponnuswamy, J. Chil. Chem. Soc.*, **2014**, *59*, 2640-2646. [Crossref], [Google Scholar], [Publisher]
[31] C.P. Tinworth, R.J. Young, *J. Med. Chem.*, **2020**, *63*, 10091-10108. [Crossref], [Google Scholar], [Publisher]
[32] W.J. Egan, K.M. Merz, J.J. Baldwin, *J. Med. Chem.*, **2000**, *43*, 3867–3877. [Crossref], [Google Scholar], [Publisher]
[33] D.F. Veber, S.R. Johnson, H.Y. Cheng, B.R Smith, K.W. Ward, K.D Kopple, *J. Med. Chem.*, **2002**, *45*, 2615-2623. [Crossref], [Google Scholar], [Publisher]
[34] I. Muegge, S.L. Heald, D. Brittelli, *J. Med. Chem*., **2001**, *44*, 1841-1846. [Crossref], [Google Scholar], [Publisher]
[35] M.A. Małkiewicz, A. Szarmach, A. Sabisz, W.J. Cubała, E. Szurowska, P.J. Winklewski, *J. Neuroinflammation*, **2019**, *16*, 15. [Crossref], [Google Scholar], [Publisher]
[36] J. Zaretzki, C. Bergeron, T.W. Huang, P. Rydberg, S.J. Swamidass, C.M. Berneman, *Bioinformatics*, **2013**, *29*, 497–498. [Crossref], [Google Scholar], [Publisher]
[37] C.A. Lipinski, J *Pharmacol. Toxicol. Methods*, **2000**, *44*, 235–249. [Crossref], [Google Scholar], [Publisher]

[38] V.B. Panchabhai, S.R. Butle, P.G. Ingole, *Research J. Pharm. Tech.*, **2021**, *14*, 3846-3854. [Crossref], [Google Scholar], [Publisher]
[39] H. Yang, C. Lou, L. Sun, J. Li, Y. Cai, Z. Wang, W. Li, G. Liu, Y. Tang, *Bioinformatics*, **2019**, *35*, 1067–1069. [Crossref], [Google Scholar], [Publisher]
[40] I.K. Shihab, M.H. Mohammed, *Iraqi J. Pharm. Sci.*, **2019**, *28*, 17-23. [Crossref], [Google Scholar], [Publisher]
[41] R.A. Khalil, H.A. Shaymaa, *Stud. U. Babes-Bol. Che.*, **2022**, *67*, 139-152. [Crossref], [Google Scholar], [Publisher]
[42] M.V. Aanandhi, J.A. Sachin, *Research J. Pharm. Technol.*, **2021**, *14*, 2191-2194. [Crossref], [Google Scholar], [Publisher]
[43] H.A. Shayma'a, R.A. Khalil, *Turkish Comput. Theor. Chem.*, **2022**, *6*, 1-8. [Crossref], [Google Scholar], [Publisher]

How to cite this article: Ali Majeed Hantoush, Zaheda Ahmed Najim, Faris T. Abachi*. Density functional theory, ADME and docking studies of some tetrahydropyrimidine-5- carboxylate derivatives. *Eurasian Chemical Communications*, 2022, 4(8), 778-789. **Link:** http://www.echemcom.com/article_147985.html